Available online at www.sciencedirect.com
SCIENCE DIRECT
Journal of Power Sources 158 (2006) 177–187
JOURNAL OF POWER SOURCES
www.elsevier.com/locate/jpowsour

Characterisation of a portable DMFC stack and a methanol-feeding concept

Anders Oedegaard *, Christian Hentschel

Fraunhofer Institute for Solar Energy Systems ISE, Heidenhofstr. 2, 79110 Freiburg, Germany

Received 24 March 2005; accepted 30 June 2005
Available online 28 February 2006

Abstract

A portable direct methanol fuel cell stack is characterised, together with a novel methanol-feeding concept. The amounts of water and carbon dioxide in the cathode and anode outlets respectively are measured and compared with calculated values based on parameters found in the literature. Due to methanol crossover, the stack temperature already increases rapidly at open circuit voltage, which also indicates substantial losses. The efficiency of the stack is found by two methods to be somewhat less than 25% at 20 W. A passive methanol supply to the feed loop is achieved by placing a permeable tube in a concentrated methanol storage tank. Diffusion of methanol through the tube walls into the methanol–water flow assures an increase in concentration. Experimental investigations of such a tube are compared with simulations.

Keywords: DMFC; Stack; Portable; Characterisation; Efficiency; Methanol feeding

1. Introduction

Fuel cells are being developed with increasing intensity to replace or support batteries in portable applications from the sub-watt range to some hundred watts. Several thousand systems have been constructed until now, and the number of actors and presented prototypes is increasing rapidly [1]. Early developers focussed mainly on hydrogen-fuelled polymer-electrolyte fuel cells (PEMFC), but during the last few years, direct methanol fuel cells have attracted more and more attention. This is principally due to the convenience of operating with a liquid fuel, which is also already available for potential consumers. Other advantages are the high energy density of methanol (MeOH) and the simple overall system design, as the complex humidification and thermal management associated with the PEMFC can be avoided [2]. In addition to companies like MTI, Toshiba, Motorola, Samsung and Smart Fuel Cells, many research institutes and universities are targeting DMFC for integration into small electrical appliances.

The performance of the direct methanol fuel cell is mostly limited by the slow redox reactions and the crossover of methanol [3]. Both the oxidation of methanol and reduction of oxygen lead to large overpotentials at the anode and cathode, respectively. In order to improve the activity of the electrodes, it is necessary to understand the reaction mechanism. Although various parallel reaction paths for the methanol oxidation are possible, there is consensus about the general course of action [2–6]. The main open question is the limiting step and the dominant adsorbed intermediate. To increase the reaction rate, catalyst loadings up to ten times higher than in PEMFC have been applied [2]. Simply due to the high costs for the precious metal, such fuel cells have no commercial potential. Therefore, much effort has been made to reduce the amount of catalyst [7] and to develop new catalysts based on cheaper materials [8–10]. For the anode, a binary catalyst consisting of platinum and ruthenium, mostly in a 1:1 atomic ratio [8], is the most common.

Due to the methanol crossover effect, the conditions at the cathode in a DMFC are very complex. The cathodic reaction of the PEMFC is well described in the literature [11], but to date there is no clear understanding of the influence of methanol on the oxygen reduction mechanism [2]. A very promising approach to avoid this problem is the development of a methanol-tolerant catalyst [12]. If this succeeds, the cathodic overvoltage will be significantly reduced, but the utilisation of methanol is

* Corresponding author. Present address: SINTEF Materials and Chemistry, Sem Sælands vei 12, NO-7465 Trondheim, Norway. Tel.: +47 94356595.
E-mail address: anders.odegard@sintef.no (A. Oedegaard).

0378-7753/$ – see front matter © 2006 Elsevier B.V. All rights reserved.
doi:10.1016/j.jpowsour.2005.06.044

Nomenclature

A	cell area (m^2)
C_j	concentration of component j ($mol\,m^{-3}$)
$C_{MeOH,mem\text{-}cat}$	methanol concentration on the membrane–catalyst interface ($mol\,m^{-3}$)
$C_{MeOH,in}$	methanol inlet concentration ($mol\,m^{-3}$)
D_j	diffusion coefficient of component j ($m^2\,s^{-1}$)
D_{MeOH,H_2O}	diffusion coefficient of methanol in water ($m^2\,s^{-1}$)
$D_{MeOH,T}$	methanol diffusion coefficient in the membrane ($m^2\,s^{-1}$)
$D_{MeOH,T_{ref}}$	methanol diffusion coefficient in the membrane at T_{ref} ($m^2\,s^{-1}$)
F	Faraday constant ($96485\,C\,mol^{-1}$)
ΔG	Gibbs energy ($kJ\,mol^{-1}$)
ΔH	enthalpy ($kJ\,mol^{-1}$)
i	current density ($mA\,cm^{-2}$)
i_{lim}	limiting current density ($mA\,cm^{-2}$)
l_{GDL}	thickness of gas diffusion layer (m)
n_{H_2O}	water drag coefficient
$n_{MeOH,y}$	methanol flux in y-direction ($mol\,s^{-1}$)
$N_{j,diff}$	diffusive flux of component j ($mol\,s^{-1}$)
$N_{j,elosm}$	electro-osmotic flux of component j ($mol\,s^{-1}$)
$N_{MeOH,ox}$	consumed methanol at the anode ($mol\,s^{-1}$)
$N_{MeOH,x}$	methanol flux in x-direction ($mol\,s^{-1}$)
$N_{MeOH,xover}$	crossover methanol ($mol\,s^{-1}$)
$N_{MeOH,y\text{-}mem}$	methanol flux in the membrane, y-direction ($mol\,s^{-1}$)
$N_{MeOH,y\text{-}tube}$	methanol flux in the tube, y-direction ($mol\,s^{-1}$)
p_{H_2O}	water saturation pressure (atm)
T	temperature (°C, K)
T_{ref}	reference temperature (K)
U_{cell}	Cell or stack voltage (V)
$U_{OCV,\Delta G}$	theoretical open circuit voltage (V)
$\dot{V}_{MeOH,H_2O,x}$	methanol–water mixture flow rate ($m^3\,s^{-1}$)
z	number of electrons

Greek symbols

η_{mass}	mass efficiency (or Faraday efficiency)
$\eta_{overall}$	overall efficiency
η_{td}	thermodynamic efficiency
$\eta_{voltage}$	voltage efficiency
χ_j	ratio of j

still low due to permeation through the membrane. The most desired solution is of course a new electrolyte, which is impermeable to methanol. DuPonts Nafion (perfluorosulfonic acid (PFSA)/polytetrafluorethylene (PTFE) copolymer in the acid form) has been the favoured membrane material for the DMFC for the last 30 years. Today much effort is put into altering its properties to reduce crossover, for instance by adding inorganic compounds such as silica (SiO_2) [13] and palladium (Pd) [14] or by physically modifying the membrane (e.g. grafting [15]) to achieve a barrier against methanol flow, without limiting the proton transport. New polymer materials, like polybenzimidazole (PBI) and polyphosphazene (PPZ), are also being investigated as alternatives to the sulfonated PFSA [2,16,17].

In addition to the restricted oxygen reduction caused by methanol, large amounts of water are present at the DMFC cathode due to the liquid anode feed and leakage through the electrolyte. Thus, the danger of flooding is quite substantial. At the same time, the wet environment is also an advantage. The liquid-fed DMFC is not limited to temperatures below 60 °C like the PEMFC if it is operated without humidification. As long as the fuel cell is fed with a liquid methanol–water solution, there is no danger of the membrane drying out. On the other hand, water leaving the cathode has to be recovered and re-injected to the anode-feeding loop. This is necessary in order to avoid a water storage tank for the DMFC system. The ideal system consists of a concentrated methanol tank, from which methanol is added to the anode feeding loop in the same amount as it is consumed on the catalyst surface. Water recovered from the cathode is returned to the same loop. If it is not possible to recover enough water, it has to be taken from an external tank, which of course leads to a lower overall energy density for the system. By keeping the methanol concentration as low as possible and avoiding a mass transportation problem on the anode, the amount of methanol lost through crossover is minimised.

In the literature there is not much published work on DMFC stack development and characterisation in the lower power range. Most of the articles are focussed on fuel cells and/or systems operating at elevated temperatures and pressures (around 100 °C and up to 3 bar) and cell areas exceeding 100 cm^2 for automotive applications and power generators around 1 kW [e.g. 18–21]. These conditions are unrealistic for portable applications, and the results obtained are not necessarily transferable to smaller cells and systems. Some preliminary results on the development of DMFC stacks in the range of 50–150 W have been presented by the Los Alamos National Laboratory (LANL) and the Jet Propulsion Laboratory (JPL). LANL assembled a five-cell stack based on 45 cm^2 cells. At 60 °C, the maximum power density was approximately 75 $mW\,cm^{-2}$ [22]. A similar stack made by JPL achieved 40 $mW\,cm^{-2}$ at 55 °C [23]. Both institutes are funded by the American DARPA military program. DMFC companies like MTI and Smart Fuel Cells are reticent in publishing details on performance and characteristics of their stacks and systems. Generally, most of the published data on DMFC under ambient conditions were obtained with small single cells [24–29].

Direct methanol fuel cells have more complicated reaction kinetics than PEMFC, and together with the influence of methanol crossover, this makes simulation more difficult than for PEMFC. However, several models have been presented recently [30–35], and the dynamic behaviour of DMFC has been investigated [18,33,34,36–39]. This better understanding of the internal and overall procedures has accelerated stack and system development.

In this paper, we present the results from the characterisation of a previously developed portable DMFC stack with respect to its performance under different operating conditions. Important

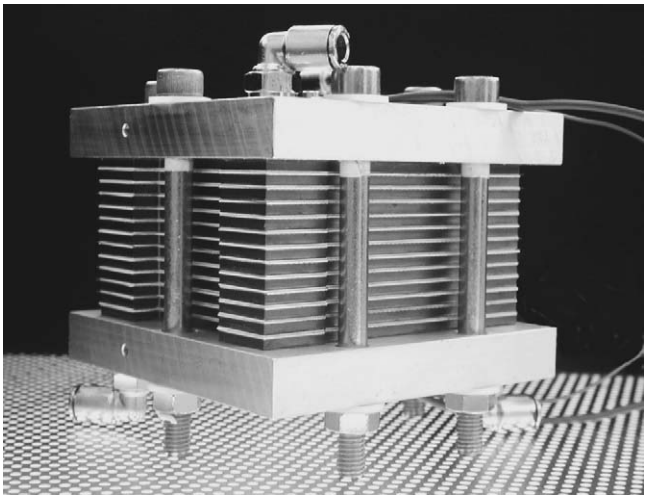

Fig. 1. The characterised 12-cell DMFC stack based on graphite bipolar plates.

data such as amounts of carbon dioxide and water and heat losses were also investigated, so the stack efficiency could be ascertained. Additionally, a novel passive methanol-feeding concept based on a Nafion® tube was characterised and compared with simulations. Finally, the stack was operated with the new feeding concept.

2. Experimental

The characterised 12-cell DMFC stack was based on graphite bipolar plates with serpentine channels on both anode and cathode. Each cell had an active area of 7 cm × 7 cm and the graphite plates were 3 mm thick. Five-layer MEAs based on Nafion® N117 membranes, with platinum–ruthenium applied on the anode and pure platinum on the cathode, were provided by a commercial supplier. Reinforced silicone foil was used for sealing. A more detailed description of the stack and its development has been given in [40]. The assembled stack is shown in Fig. 1.

All experiments were performed with ambient air at ambient pressure on the cathode side. Air was fed by a membrane pump with a maximal air flow of 5 l min^{-1}. Methanol was supplied by a pulse-free micro-dosing pump. When the stack was operated at elevated temperatures, the methanol–water mixture was preheated before entering the stack. Isothermal operation of a stack is difficult to maintain as the produced heat rapidly increases with current density. A substantial part occurs due to the crossover effect. In addition to the total stack current and voltage, the single cell voltages were recorded as well. Each point in the polarisation curves was measured for 5 min before recording the data. The standard test conditions, if not specified otherwise, were flow rates of 60 ml min^{-1} for 1 M MeOH and 4.7 l min^{-1} for air, and operation at 50 °C.

3. Stack performance

From the initial testing of the stack, it was found to be almost impossible to operate at high current densities without pulsed air flow [40]. This was due to the poor and inhomogeneous water removal from the cathodes. However, when operated with a membrane pump, the stability and the maximum performance improved drastically. The pressure drop of the stack was measured to be 30 mbar at 4.5 l min^{-1} under dry conditions.

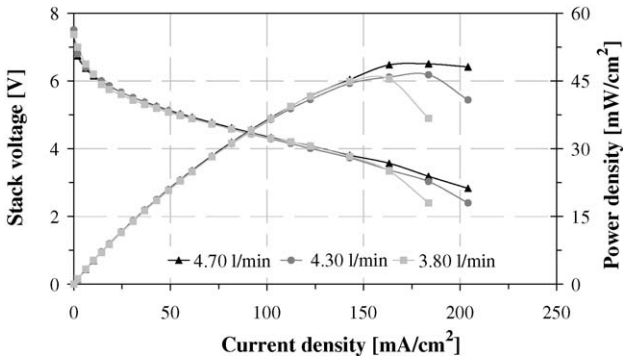

Fig. 2. Influence of different air flow rates at 50 °C and 1 M MeOH at 60 ml min^{-1}.

3.1. Influence of flow rates

Due to water and methanol crossover, large amounts of water are present at the cathode. At low temperatures and thus low water saturation pressures, this leads to formation of droplets in the cathodic flow-fields and manifolds of the stack. The influence of the air flow rate on the water removal with 1 M MeOH at 60 ml min^{-1} and 50 °C is shown in Fig. 2. Tests with 3.8, 4.3 and 4.7 l min^{-1} was performed. At 200 mA cm^{-2} (or almost 10 A overall stack current), the stoichiometric air flow rate is about 2.2 l min^{-1}. In the lower current density region, no significant difference is observed between the curves. The air flow rate does not affect the performance until the current density is higher than 150 mA cm^{-2}. Usually this behaviour is related to mass transport problems, either oxygen starvation or water flooding. Drying out of the membrane as in hydrogen-fuelled PEMFC is highly unlikely. Both the air flow rates of 3.8 and 4.3 l min^{-1} are too low to maintain high performance.

Without considering the parasitic consumption due to methanol crossover, the oxygen in 3.8 l min^{-1} of air is still more than twice the amount reduced at the cathode at 150 mA cm^{-2}. However, according to measurements presented by Gogel et al. and Ren et al., the equivalent current densities resulting from methanol crossover can be as high as 50–100% of the cell current [22,28]. This could indicate that there is a possibility of oxygen starvation. In Fig. 3, the single cell voltages corresponding to the polarisation curve with 3.8 l min^{-1} air are shown. Already at low current densities, there is a difference of 30 mV between the best and the worst cell. This difference increases continuously, until one single cell voltage drops drastically as the current is raised to 140 mA cm^{-2}. By increasing the current even more, several cell voltages start to oscillate. A similar effect has previously been described in single cells [40], with the conclusion that the behaviour was caused by the removal of water droplets from the cathode flow-field channels.

If oxygen starvation was the main problem, all the cell voltages should have decreased more simultaneously. Thus, it is

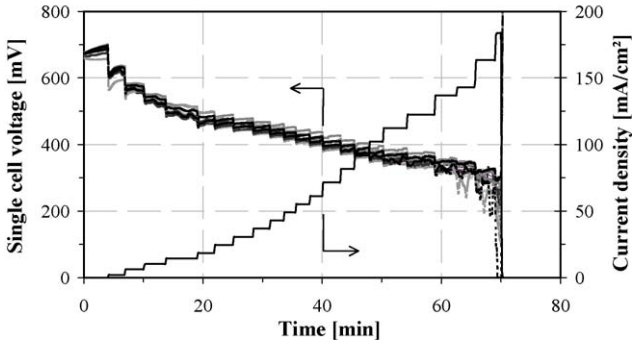

Fig. 3. Single cell voltages during measurement of polarisation curves with 3.8 l min^{-1} air as shown in Fig. 2.

more likely that some cells have difficulties with the removal of water from the cathode. A uniform distribution of air to all cells and removal of water from them is not easy to assure, and those with the lowest flow rate limit the total stack performance. Since the effective oxygen stoichiometry could be lower than two, this certainly also influences the stack. By increasing the flow rate the performance improves, but this increases the parasitic power consumption and increases the water losses at the same time.

Analogous to water production at the cathode, carbon dioxide is produced at the anode. Effective removal is equally important to obtain stable and good performance. Methanol is fed to the stack as a methanol–water mixture at much lower volumetric flow rates than air. The difficulty with even distribution to all cells was demonstrated with air, where an increased flow rate improved the homogeneity. At 200 mA cm^{-2}, the stoichiometric flow rate of 1 M methanol is 12 ml min^{-1}; considering the methanol crossover, it could be around 20–25 ml min^{-1}. The dependence of flow rates between 50 and 80 ml min^{-1} is shown in Fig. 4. For all cases, the amount of methanol is well above the stoichiometric rate, nevertheless in the 50 ml min^{-1} test the voltage in one cell dropped immediately as the current was increased. It was only possible to operate at higher current densities with higher flow rates, thus the fuel distribution improved the same way as with air. Experience from similar single cell testing with high stoichiometric flow rates reveals no significant direct influence of the methanol–water flow rate. With a serpentine shaped anode flow-field, the CO_2 removal from a single cell is usually no problem. As the number of cells in a stack increases, the fuel distribution between cells becomes more difficult [24].

The poorer performance of the stack at flow rates higher than 60 ml min^{-1} must be considered in combination with the experimental set-up. In order to start at 50 °C, the methanol–water mixture is preheated before entering the stack. During operation, the stack temperature increases even more due to efficiency losses, mainly combustion of crossover methanol at the cathode. At some point, the temperature of the methanol–water mixture is lower than the stack, and then no longer heats the stack, but cools it. The higher the flow rate, the greater is the cooling effect, and thus the decrease in performance. In an autonomous system, a similar situation will arise because the feeding loop will have a lower temperature than the stack most of the time.

3.2. Influence of methanol concentration and temperature

Another important factor in direct methanol fuel cells is the methanol concentration in the anode feed. According to the oxidation kinetics of methanol, the ideal methanol–water molar ratio should be 1:1. Due to the crossover phenomenon, the methanol concentration is usually much lower, around 1 M, which corresponds to approximately 1:25. Higher concentrations lead to more methanol on the cathode side. In addition to a reduced cell/stack voltage caused by the mixed potential (methanol/oxygen), more water at the cathode reduces the access of oxygen to the catalyst. Two water molecules are formed by complete combustion from each crossover methanol molecule. At lower concentrations, the open circuit voltage (OCV) is higher, but then the stack also experiences mass transport problems earlier because of methanol starvation. The performance of the stack operated with different methanol concentrations is shown in Fig. 5.

The results with the 12-cell stack show the same trend as with small single cells. The OCV sinks with increasing methanol concentration, and the limiting current densities increase. At some point the maximum is reached, and the performance starts to decrease when the concentration is further increased. Due to the large amounts of water at the cathode, the single cell voltages

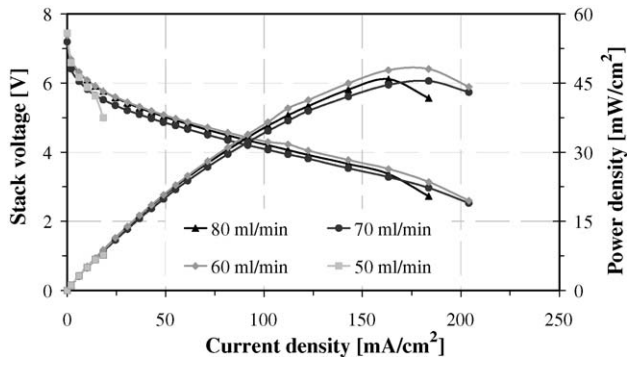

Fig. 4. Influence of different methanol–water flow rates with 1 M MeOH, at 50 °C and 4.7 l min^{-1} ambient air.

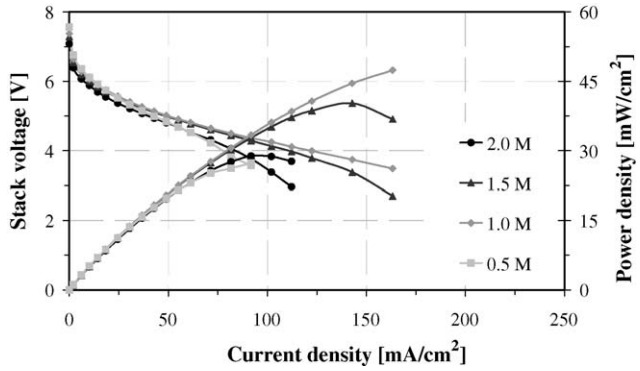

Fig. 5. Effect of varying the methanol concentration in the anode feed. Methanol flow rate 60 ml min^{-1}, 50 °C and ambient air at 4.7 l min^{-1}.

are much more unstable when a high methanol concentration is used, mainly due to the lower cathode potential. The voltage oscillations seen in Fig. 3 around 150 mA cm^{-2} already begins at 60 mA cm^{-2} in the 2 M test. The 1 M test showed the highest performance of all the investigated methanol concentrations. This is, as we mentioned before, the most common value. Kulikovsky has found the optimal MeOH concentration to be 0.97 M by modelling the current–voltage curve of a DMFC [41].

The situation in a stack is somewhat more complicated compared to single cells. With the larger inlet and outlet manifolds and longer flow-field channels, the amounts of accumulated water and carbon dioxide cause inhomogeneous conditions in the stack, especially at the cathode. Additionally, the temperature effect of methanol crossover is notable. It was mentioned above that the amount of crossover methanol might be as much as 100% of the methanol oxidised at the anode. If the efficiency of a 30 W stack itself, without considering crossover, is 50%, the total heat production in the same could be around 90 W. This is dependent on the methanol concentration, and thus operating with different concentrations leads to different stack temperatures. Up to 20 K difference in the stack temperature was measured between the 0.5 and 2.0 M operation during the measurements shown in Fig. 5.

An increase in temperature primarily has a positive impact on the reaction kinetics. At the same time, the crossover of both water and methanol increases [42]. When tested at different temperatures, the low current density part of the stack's polarisation curve improves significantly with rising temperature, see Fig. 6. This part of the plot corresponds to kinetic limitations. Throughout these measurements, the stack temperature could not be kept entirely constant, which resulted in an increase of up to 10 K during the polarisation curves.

The poor performance at 80 °C has essentially nothing to do with the boiling point of pure methanol at 64 °C. Through all of the experiments, the anode feed remained in the liquid state, since the 1 M methanol–water mixture boils close to 100 °C. Both the electro-osmotic drag and diffusion of methanol and water are dependent on the temperature. In this case, this leads to critical amounts of water at the cathode, and the air flow rate is not sufficient to prevent flooding. Ren et al. reported the same findings at high temperatures for liquid-fed DMFC [43]. Just before the temperature is high enough to remove cathode water

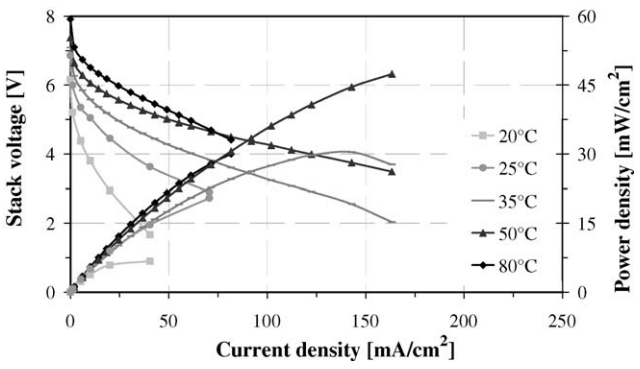

Fig. 6. Effect of varying the stack temperature with 1.0 M methanol at 60 ml min^{-1} and ambient air at 4.7 l min^{-1}.

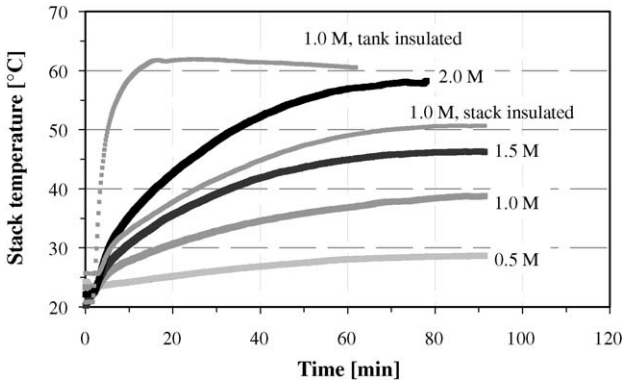

Fig. 7. Effect of methanol concentration and insulation of stack and tank on stack temperature at OCV. Methanol–water mixture at 60 ml min^{-1} and ambient air at 4.7 l min^{-1}.

by evaporation in the channels, the danger of flooding is at its maximum.

3.3. Influence of methanol crossover and insulation of stack and methanol tank

In the measurements presented above, the stack performance showed a strong dependence on methanol concentration and operating temperature. It was also seen that different stack temperatures resulted from varying the methanol concentration, despite efforts to keep the stack under isothermal conditions. The correlation between methanol concentration and stack temperature is shown in Fig. 7 below. The stack temperature was recorded during open circuit operation with different methanol concentrations and insulation of the methanol tank and the stack itself. The temperature stabilises in most cases within 75 min from start-up. When the concentration is increased from 0.5 to 2.0 M, the stack temperature at OCV rises from 29 to 58 °C, a difference of almost 30 K. This is due to the methanol crossover and direct oxidation at the cathode. For each mole of methanol diffusing through the membrane, 726 kJ of energy is released during the cathodic combustion [44]. Thus, the temperature of both the methanol–water mixture and the stack itself increases until the heat of combustion equals the heat removal by fuel flow and thermal radiation from the stack.

Another way to increase or keep the operating temperature as high as possible is to insulate the stack and the methanol–water fuel tank. During experiments with a thermally insulated stack, the temperature was considerably higher than without insulation. Over 50 °C was reached compared to 39 °C in the non-insulated case with a 1 M methanol solution. At the beginning of each test, the methanol–water mixture (5 l) was at room temperature. Since the fuel was pumped in a loop, the temperature of the fuel in the tank increased as the temperature of the stack increased. In order to minimise the heat losses in the fuel tank and piping, they may be insulated as well as the stack. To evaluate the performance of a system with complete insulation of the tank and piping, the methanol–water mixture was heated to 60 °C before entering the stack. This was in the temperature range, which could be reached in the stack during operation without heating and insulation. If

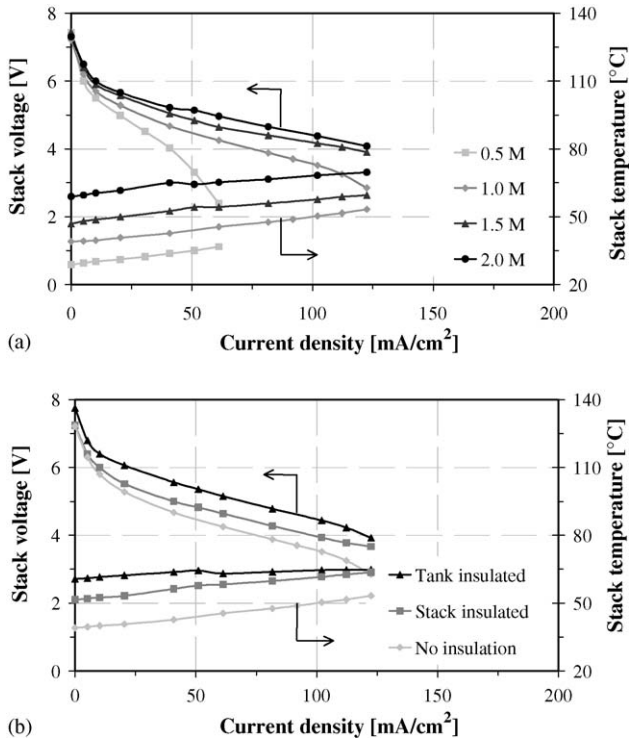

Fig. 8. Performance and temperature of the stack for different methanol concentrations (a) and insulation of stack and tank (b). Methanol–water mixture at 60 ml min^{-1} and ambient air at 4.7 l min^{-1}.

the fuel storage tank is insulated well enough, it is not unlikely that the fuel might reach the same temperature.

The measurements in Fig. 7 are also interesting with regard to start-up procedures for DMFC. As shown in Fig. 6, the stack performance is highly dependent on temperature, and for the efficiency it is important to achieve a high operating temperature as quickly as possible. This can be done both by insulating the stack and the fuel tank, and by operating with a higher methanol concentration during the first minutes. In case cooling of the system is needed, insulation of the stack is not advantageous.

In Fig. 8, the polarisation curves taken after the measurements shown in Fig. 7 are presented. Additionally, the stack temperature is plotted in the same diagrams. The difference in conditions between the plots in Fig. 8(a) and Fig. 5 is the temperature control of the stack. At non-isothermal operation, the influence of methanol concentration is more complex due to the effect of methanol crossover on temperature. Operation with 2 M methanol performs better than with 1 M due to the 15 °C higher stack temperature. However, long-term operation with high concentration is not desired due to efficiency losses. As noted earlier, the single cell voltages are more unstable during operation with a high methanol concentration, which indicates more water in the cathode flow-field channels. Fig. 8(b) shows the effect of insulating the stack and the fuel tank. Here, also the difference between the curves is due to temperature variations. Since it is valuable to have the option to cool the stack by a fan, the best option would be to insulate the fuel tank and piping.

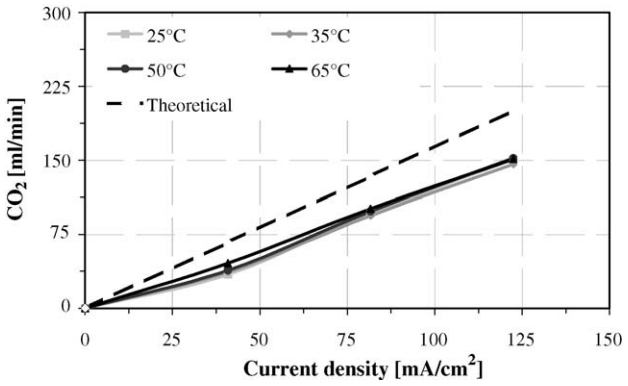

Fig. 9. Measured and calculated amounts of CO_2 in the anode outlet at different temperatures.

3.4. Carbon dioxide, water and heat

From the total DMFC reaction equation (Eq. (1)), the amounts of produced carbon dioxide and water can be calculated.

$$CH_3OH + 3/2O_2 \rightarrow CO_2 + 2H_2O \quad (1)$$

However, due to mass transport of water, methanol and CO_2 through the electrolyte, the experimental results deviate considerably from the theoretical values. The transport mechanisms can be described by Fick's diffusion and electro-osmotic drag [40,45], and thus be included in the calculated amounts of water, methanol and CO_2. Fig. 9 presents both the measured and theoretical amounts of produced carbon dioxide from the anode at different operating temperatures. At 120 mA cm^{-2}, the measured value only accounts for about 75% of the theoretical one. This can be explained by incomplete oxidation of methanol. The anode reaction mechanism consists of multiple steps and involves several intermediate products. Earlier results have shown traces of formaldehyde, formic acid, methyl formate and methylal in the anode outlet [4,11,46]. From the experiments done here, it can be seen that the amount of CO_2 increases with temperature, which correlates with a higher conversion rate at elevated temperatures. Carbon dioxide may also diffuse through the polymer membrane to the cathode side. Dohle et al. reported amounts as high as 20% of the CO_2 produced on the anode side at 100 mA cm^{-2} and high temperature [47]. Our mass spectroscopy results from half-cell tests with identical MEAs correspond to about 7 ml min^{-1} carbon dioxide for the stack at these operating conditions. Thus, we assume that the main reason for the deviation between measured and theoretical value is the partial conversion of methanol. More data from the mass spectroscopy investigations will be presented in another paper.

During measurement of the polarisation curves, the temperature in the stack increased, and deviated in some cases strongly from the initial value (the one given in Fig. 9), see Table 1. As mentioned before, this is due to heat, which evolved as a result of different efficiency losses throughout operation. Since the actual stack temperatures at high current densities are similar, there are not large differences between the CO_2 curves. The same carbon dioxide measurements were made with different methanol concentrations as well, and, as expected, no variations were found.

Table 1
Measured stack and air outlet temperatures during operation (°C)

Initial temperature	Stack temperature at [mA cm^{-2}]				Air out temperature
	0	40	80	120	
25	33	39	46	52	26–37
35	41	45	49	52	31–41
50	55	58	60	62	37–43
65	67	68	69	71	49–52

Throughout the CO_2 experiments described above, the amounts of liquid water in the cathode outlet flow were also collected and measured. Due to the liquid anode feed and the crossover phenomenon, considerably more water is found at the cathode of a DMFC than of a PEMFC. The measured quantity of water consists of produced water, according to the cathodic reduction of oxygen, as well as diffusion and electro-osmotic drag of water and methanol from the anode. Methanol on the cathode is immediately oxidised to water and carbon dioxide [48]. Furthermore, the humidity of the inlet and outlet airflows has to be considered. Under these operating conditions, it may be assumed that the outlet air is totally saturated with water. Diffusion through the membrane is described by Fick's diffusion:

$$N_{j,\mathrm{diff}} = -D_j \frac{\partial C_j}{\partial x} \tag{2}$$

Most publications in this field give a methanol diffusion coefficient of around $1 \times 10^{-9}\,\mathrm{m^2\,s^{-1}}$ [26,49,50]. The temperature dependence of the coefficient is said to follow the equation used by Shimpalee and Dutta for the water diffusion coefficient [51]:

$$D_{\mathrm{MeOH},T} = D_{\mathrm{MeOH},T_{\mathrm{ref}}} \exp\left[2416\left(\frac{1}{T_{\mathrm{ref}}} - \frac{1}{T}\right)\right] \tag{3}$$

Due to the large amounts of liquid present at the cathode, diffusion of water is initially considered to be negligible. Results presented by Müller [52] indicate that this assumption is valid at temperatures below 80 °C. The amount of water and methanol dragged from the anode to the cathode depends on the current density, the cell area, the water drag coefficient and the molar ratio of water/methanol at the membrane–catalyst interface [41]:

$$N_{j,\mathrm{elosm}} = \frac{iA}{F} n_{\mathrm{H_2O}} \chi_j \tag{4}$$

In a membrane equilibrated with water, the drag coefficient varies from 2 to 5 according to the literature [30,42,47]. The majority of the presented data are gained by using a Nafion® N117 membrane, but discrepancies may arise due to different catalyst coating methods, catalyst amounts and gas diffusion layer (GDL) properties as well as differences in other hardware components. The methanol concentration is assumed to decrease linearly from the anode flow channel to the membrane–catalyst interface. At the limiting current density, the concentration is zero.

$$C_{\mathrm{MeOH,mem\text{-}cat}} = C_{\mathrm{MeOH,in}}\left(1 - \frac{i}{i_{\mathrm{lim}}}\right) \tag{5}$$

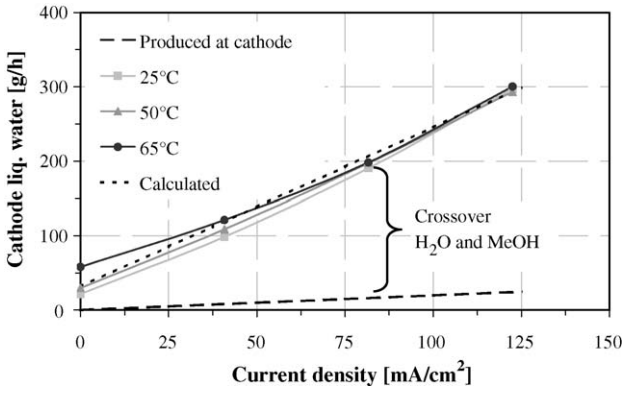

Fig. 10. Measured and calculated amounts of water in the cathode outlet at different temperatures. The calculations were made for operation at 50 °C.

Table 2
Calculated and measured amounts of water in the cathode outlet at OCV

Test conditions	1.0 M (25 °C)	1.0 M (50 °C)	1.5 M (50 °C)	1.0 M (65 °C)
Measured water (g h^{-1})	21.6	29.6	45.7	58.1
Calculated water (g h^{-1})	20.4	29.3	45.5	55.5

By applying Faraday's equation and an effective diffusion coefficient in the GDL, the limiting current can be calculated:

$$i_{\mathrm{lim}} = D_{\mathrm{MeOH,GDL,eff}} \frac{zFC_{\mathrm{MeOH,in}}}{l_{\mathrm{GDL}}} \tag{6}$$

This effective diffusion coefficient was found to be $1.6 \times 10^{-9}\,\mathrm{m^2\,s^{-1}}$ at 50 °C from fitting to single-cell experimental results. The same type of MEAs and operating conditions as in the stack testing were used. Furthermore, the GDL diffusion coefficient follows the same temperature dependence as the membrane diffusion coefficient, see Eq. (3).

For the calculation of water in the inlet and outlet airflows, the fitted equation for temperature-dependent water saturation pressure presented by Springer et al. was used [45][1]:

$$p_{\mathrm{H_2O}} = 10\exp(-2.1794 + 0.2953T - 9.1837 \times 10^{-5}T^2 + 1.4454 \times 10^{-7}T^3) \tag{7}$$

Both the inlet and outlet temperatures of the stack were measured and used in the calculations. Fig. 10 shows the amounts of water found during operation at different temperatures. A methanol diffusion coefficient of $1.0 \times 10^{-9}\,\mathrm{m^2\,s^{-1}}$ at 50 °C and a water drag number of 5 were adopted for the calculations. Most astonishing is the relationship between the water produced by "useful" oxygen reduction and the total amount at the cathode. At 100 mA cm^{-2} the ratio is even less than 1:10. In the low current density region, the influence of temperature on diffusion is seen. Table 2 shows measured and calculated amounts of water at open circuit voltage. The calculations are based on the equations presented above (Eqs. (2)–(7)). The temperatures and the methanol concentrations are the only variable input param-

[1] This equation is based on temperature in °C and pressure in atm.

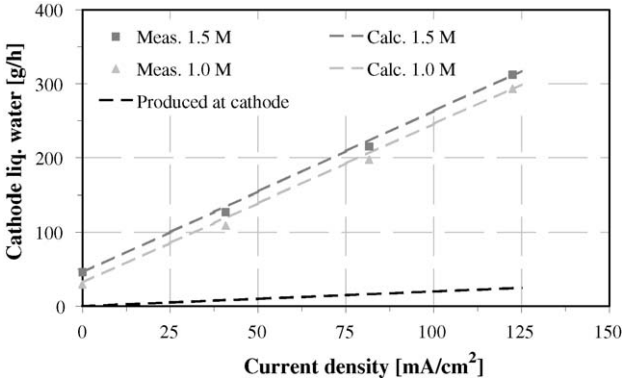

Fig. 11. Measured and calculated amounts of water in the cathode outlet for different methanol concentrations.

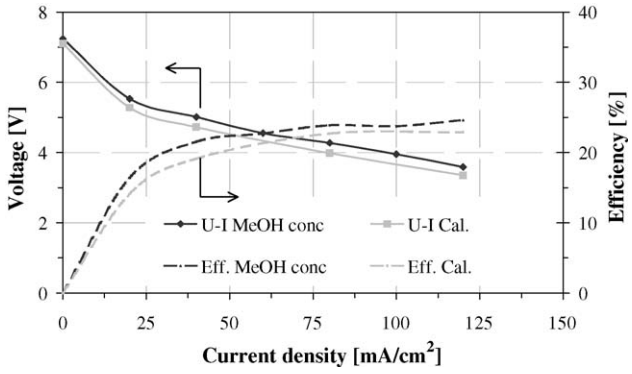

Fig. 12. Measured efficiency of the stack at 50 °C, 1 M MeOH 60 ml min^{-1}, 4.7 l min^{-1} air.

eters. As the current increases, the curves form straight lines, indicating that the electro-osmotic drag is dominating. Due to the non-perfect isothermal operation and the resulting increase in stack temperature, as shown in Table 1, all curves approach each other at higher currents.

In Fig. 11, the effect of a higher methanol concentration is seen. According to Eqs. (2) and (4), both diffusion and electro-osmotic drag of methanol through the membrane increases. The corresponding decrease in water concentration is relatively small and an effect should not be detected. However, 2 mol of water are formed on the cathode from one extra mole of crossover methanol. Already an increase in concentration from 1.0 to 1.5 M gives a noticeable increase in the amount of water. During the investigation of the effect of varying methanol concentrations, see Fig. 5 and Fig. 8(a), the increased single-cell voltage oscillation was explained by more water in the cathode flow-fields during operation with high concentrations. The results presented in Fig. 11 justify this statement. Generally, the calculated values agree well with the experimentally found ones, so the water and methanol transport can well be described by the "simplified" equations and parameters above. Diffusion of water at low temperatures is negligible compared to electro-osmosis and water from methanol diffusion, as also found in [52].

Methanol crossover is followed by a decrease in the mass efficiency. At low current densities, the effect of diffusion and electro-osmotic drag of methanol dominates the overall efficiency due to parasitic fuel oxidation at the cathode [20]. Together with the other operating losses, this is turned into heat. The overall efficiencies of the DMFC stack were ascertained by applying two different approaches. First, the mass (or Faraday) efficiencies found by measuring the methanol concentration in the anode outlet at varying current densities were used together with the voltage and the thermodynamic efficiencies, see Eq. (8) and Table 3.

$$\eta_{\text{overall}} = \eta_{\text{td}}\eta_{\text{mass}}\eta_{\text{voltage}} = \frac{\Delta G}{\Delta H}\frac{N_{\text{MeOH,ox}}}{N_{\text{MeOH,ox}} + N_{\text{MeOH,xover}}}\frac{U_{\text{cell}}}{U_{\text{OCV},\Delta G}} \quad (8)$$

These values were compared with efficiencies found by using a calorimetric method. In this method, the stack was operated in an insulated water container, while the temperatures of the air and methanol–water flows, stack and water in the container were recorded. Three liters of water were heated to the temperature of the operating stack and added to the container. In preliminary investigations, the heat losses from the container to the surroundings were found to be 5 W as long as the temperature of the water in the container was around 50–60 °C. The heat capacity of the stack was also determined before the tests. An enthalpy balance of the anode and cathode flows combined with the heat absorbed in the water and the stack gave the total heat losses during operation. Thus, the overall efficiency could be calculated. Fig. 12 shows the polarisation curves as well as the stack efficiencies for both methods.

Generally, the thermodynamic efficiency for fuel cells is very high. For DMFC operating under these conditions, it is 96%. The mass efficiency is dependent on the methanol crossover, and thus increases with current density. At 100 mA cm^{-2} it is over 80%, similar to values presented in the literature, e.g. by Müller [52]. Traces of methanol at the cathode lead to a mixed potential, and this is responsible for the low voltage efficiency, of approximately 30–50%. Combining all effects, the stack efficiency reaches its maximum just below 25%, somewhat higher than previously published data on comparable single cells [23] and stacks [53], which were both less than 20%. The poor overall efficiency at low current densities is due to the low mass efficiency. Without adjusting the methanol concentration to the consumption at the anode, dynamic operation of DMFC will

Table 3
Methanol concentration in anode outlet at different current densities

	Tank concentration	Current density [mA cm^{-2}]						
		0	20	40	60	80	100	120
MeOH concentration (M)	1.030	0.994	0.979	0.960	0.941	0.922	0.904	0.898

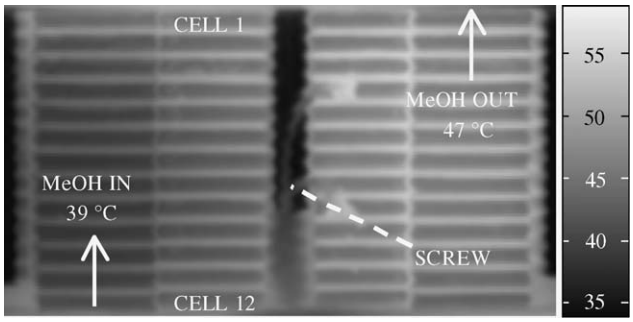

Fig. 13. Side view infrared image of the stack at 120 mA cm^{-2}, 1 M MeOH 60 ml min^{-1} and 4.7 l min^{-1} air. See also Fig. 1.

lead to very inefficient operation. The PEMFC, however, does not suffer from crossover and therefore has a much higher efficiency for partial loads.

With a power output of 30 W and an overall stack efficiency of 25%, 90 W of heat is produced. Since most of the heat is absorbed by the methanol–water flow, this leads to an in-homogeneous temperature distribution from the inlet to the outlet as seen in Fig. 13. The figure shows a side view infrared image, taken of the DMFC stack during operation at 120 mA cm^{-2}, see also Fig. 1. Methanol enters the stack at the bottom left, and exits from the top right. The anode feed is not heated before entering the stack. A temperature difference of almost 10 K arises between the inlet and outlet anode manifolds.

4. Passive methanol feeding

The methanol–water mixture usually flows in a loop between the stack and tank. Both water and methanol are consumed at the anode, and at some point they have to be added to the tank. From the DMFC reaction equation we can see that the water balance is positive. As long as enough water is recovered from the cathode air outlet, no extra tank is required. Methanol, however, should be stored in as pure a form as possible in order to guarantee a high energy density of the system. The simplest design is to have two tanks; one small "operating" tank with diluted methanol, where the recovered water is injected, and one larger concentrated methanol storage unit for methanol refill to the feed loop. This design requires one extra liquid pump. To reduce the parasitic power consumption, a passive solution would be preferred. By applying a methanol-permeable material, fuel can be added by means of diffusion. Fig. 14 presents a passive methanol feeding concept based on a Nafion® tube immersed in a tank filled with concentrated methanol. The diluted methanol flows inside the tube, whereas methanol is continuously added from the tank. At the same time, methanol is consumed in the stack.

Methanol transport can be described by Fick's diffusion of methanol through the membrane, with the same equations and parameters as presented above. The steady-state mass balance for methanol in the tube is given by:

$$0 = \frac{\partial N_{\mathrm{MeOH},x}}{\partial x} + \frac{\partial N_{\mathrm{MeOH},y}}{\partial y} \tag{9}$$

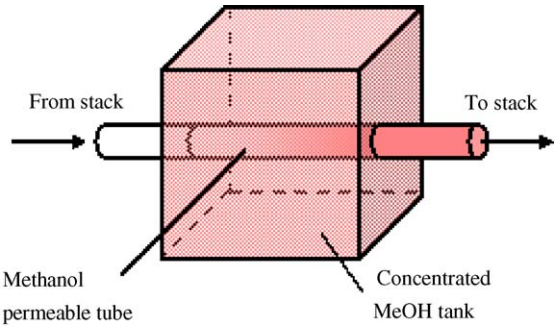

Fig. 14. A passive methanol feeding concept.

In the y-direction, only diffusion of methanol takes place:

$$N_{\mathrm{MeOH},y\text{-mem}} = -D_{\mathrm{MeOH},T}\frac{\partial C_{\mathrm{MeOH}}}{\partial y} \tag{10}$$

where the methanol diffusion coefficient is the same as in Eq. (3). Further assumptions and simplifications for the calculations are that only methanol transport through the membrane is considered and the concentration drop in the methanol storage tank is assumed to be negligible for short-term operation.

Experiments were performed with a Nafion® tube TT-070, with an inner tube radius of 0.76 mm and wall thickness of 155 μm in the dry state. When exposed to methanol, the material swells up to 130% of its original size. Pure water was pumped through the tubes, and the methanol concentration of the liquid was determined by density measurement. Fig. 15 shows both the measured and simulated methanol concentrations, as points and lines, respectively.

The dependence of the outlet methanol concentration on the chosen parameters was as expected; a decrease with liquid flow rate and an increase with tube length, temperature and inlet methanol concentration. Due to the large methanol concentration drop over the membrane, the increase in outlet concentration was independent of the inlet concentration range investigated. The simulated values are almost identical to the experimental results under these conditions. Since the DMFC is independent of methanol flow rate to some degree, this can be used to regulate the methanol concentration in the feed.

5. Operation of stack with passive methanol feeding

A simple system based on the passive methanol-feeding concept would consist of two pumps, one for air and one for the methanol–water cycle. To recover the cathode water, the air outlet is connected to the methanol–water tank, see the system sketch in Fig. 16.

In Table 3, the methanol outlet concentration at 100 mA cm^{-2} was given as 0.9 M. Based on the above measurements and simulations, it was calculated that a 20 cm (dry) tube of the same kind would be sufficient to increase the methanol concentration to around 1.0 M at 60 ml min^{-1} and 35 °C. A test set-up like the one shown in Fig. 16 without water recovery was constructed. Fig. 17 shows the stack voltages and temperatures for the passive concept and normal feeding with 1 M methanol during a 40 min period of operation. Both the temperature and

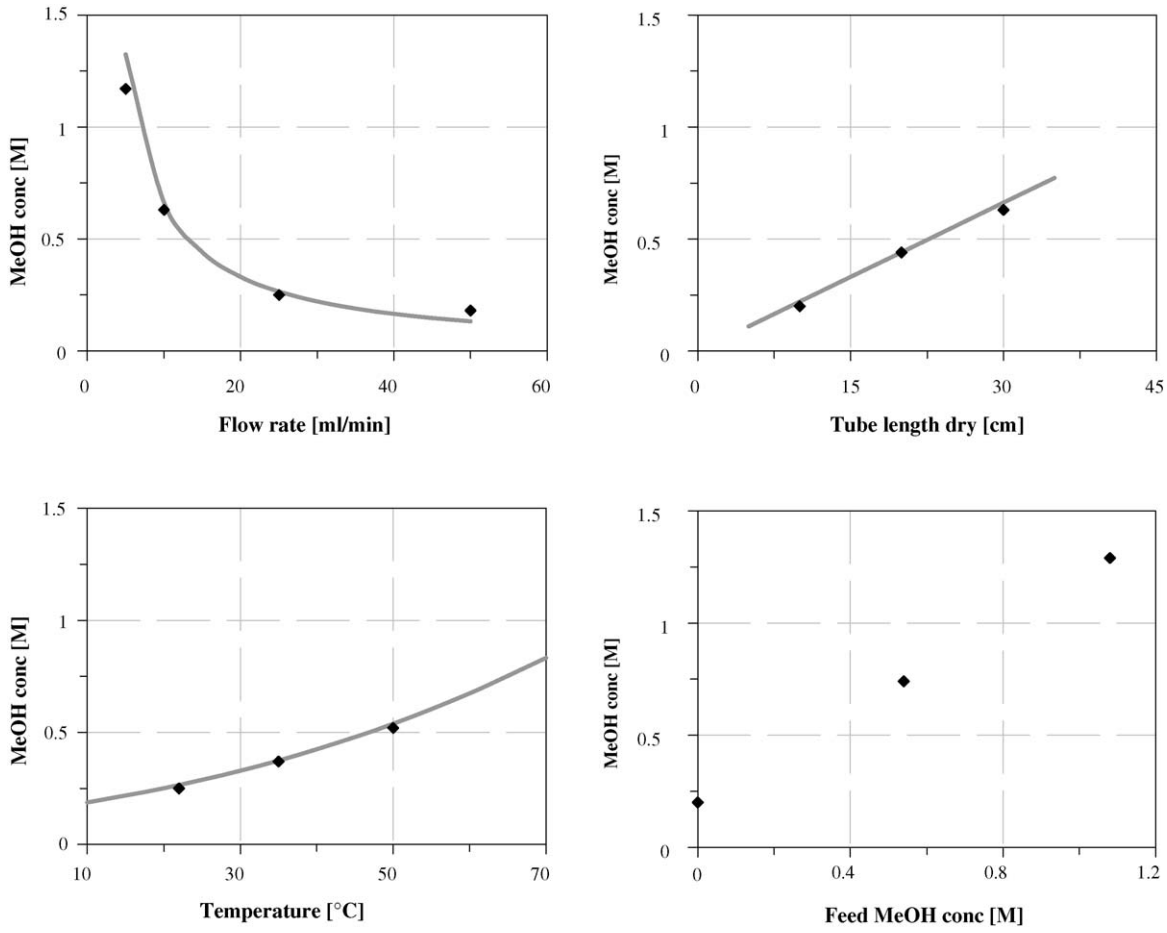

Fig. 15. Simulated (lines) and measured (points) methanol concentrations with Nafion® tube TT-070.

voltage are somewhat lower with the passive methanol feeding method. Due to degradation of the stack, the total power at 100 mA cm^{-2} had dropped from 20 W to about 16 W at the time when these experiments were performed. The same test with a 10 cm tube failed because the methanol concentration was too low.

Due to water diffusion through the tube wall, the methanol concentration in the tank sinks with time. This means that less methanol is added to the anode feed flow. To exploit the complete amount of fuel in the tank, solutions on how to lead the methanol directly from the tank to the anode feed loop have to be developed. By applying valves this can still be done without much power consumption.

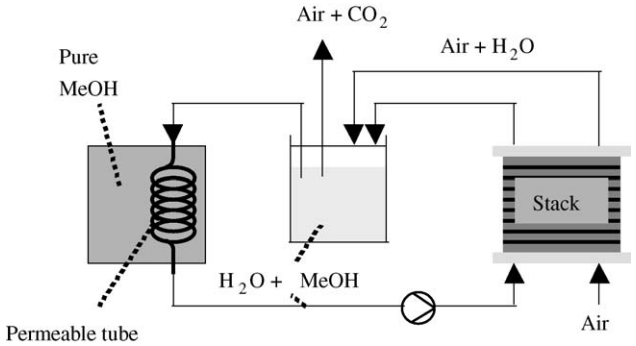

Fig. 16. Schematic design of DMFC stack with passive methanol feeding.

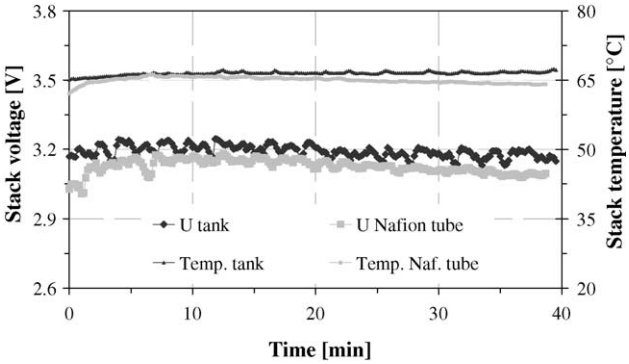

Fig. 17. Stack voltage and temperatures at 100 mA cm^{-2} during operation from 1 M MeOH tank and methanol addition through a 20 cm Nafion® tube.

6. Conclusion

A thorough characterisation of a small DMFC stack and a methanol-feeding concept have been presented. The main important operating parameters are the air flow rate, the methanol concentration and the stack temperature. Insulation of the methanol–water tank and piping reduces the heat losses and

improves the start-up behaviour by increasing the temperature. Measured amounts of water in the cathode outlet agree well with calculated data based on diffusion and electro-osmotic drag of water and methanol through the membrane. On the other hand, a difference between the measured and calculated amounts of carbon dioxide at the anode indicates that the methanol oxidation on the anode is not complete. This affects the already low efficiency, here measured to be around 25% for the stack.

Due to the liquid methanol fuel, it is possible to feed with dry air at temperatures above 60 °C without drying out the membrane. For optimal performance it is desired to operate at the highest practical temperature, while still retaining liquid operation. Thus, the efficiency losses should be exploited to heat the stack during start-up and keep the temperature stable and high during operation. The insulation experiments showed that insulation of the fuel tank and piping are most effective.

A passive method to add methanol to the methanol–water mixture was also presented and tested. The "passive" stack operation was comparable to "normal" 1 M methanol operation. In general, loss of methanol due to crossover and water in the cathode outlet still remain major hurdles to efficient DMFC systems.

References

[1] M. Cropper, Proceedings of the Fuel Cell World 2003, Lucerne, Switzerland, 2003, pp. 43–54.
[2] R. Dillon, S. Srinivasan, A.S. Aricò, V. Antonucci, J. Power Sources 127 (2004) 112–126.
[3] P. Costamagna, S. Srinivasan, J. Power Sources 102 (2001) 242–252.
[4] S. Wasmus, A. Küver, J. Electroanal. Chem. 461 (1999) 14–31.
[5] A. Hamnett, Catal. Today 38 (1997) 445–457.
[6] M.P. Hogarth, T.R. Ralph, Platinum Met. Rev. 46 (49) (2002) 146–164.
[7] A.S. Aricò, V. Baglio, E. Modica, A. Di Blasi, V. Antonucci, Electrochem. Commun. 6 (2004) 164–169.
[8] E. Antolini, Mater. Chem. Phys. 78 (2003) 563–573.
[9] Z. Wei, S. Wang, B. Yi, J. Liu, L. Chen, W.J. Zhou, W. Li, Q. Xin, J. Power Sources 106 (2002) 364–369.
[10] W.C. Choi, J.D. Kim, S.I. Woo, Catal. Today 74 (2002) 235–240.
[11] A. Hamnett, Handbook of Fuel Cells, vol. 1, John Wiley and Sons Ltd., Chichester, United Kingdom, 2003 (Chapter 18).
[12] R.W. Reeve, P.A. Christensen, A.J. Dickinson, A. Hamnett, K. Scott, Electrochim. Acta 45 (2000) 4237–4250.
[13] P.L. Antonucci, A.S. Aricó, P. Creti, E. Ramunni, V. Antonucci, Solid State Ionics 125 (1999) 431–437.
[14] W.C. Choi, J.D. Kim, S.I. Woo, J. Power Sources 96 (2001) 411–414.
[15] K. Scott, W.M. Taama, P. Argyropoulos, J. Membr. Sci. 171 (2000) 119–130.
[16] A. Heinzel, V.M. Barragán, J. Power Sources 84 (1999) 70–74.
[17] J.A. Kerres, J. Membr. Sci. 185 (2001) 3–27.
[18] P. Argyropoulos, K. Scott, W.M. Taama, Chem. Eng. J. 73 (1999) 217–227.
[19] D. Buttin, M. Dupont, M. Straumann, R. Gille, J.-C. Dubois, R. Ornelas, G.P. Fleba, E. Ramunni, V. Antonucci, A.S. Aricó, P. Creti, E. Modica, J. Appl. Electrochem. 31 (2001) 275–279.
[20] H. Dohle, H. Schmitz, T. Bewer, J. Mergel, D. Stolten, J. Power Sources 106 (2002) 313–322.
[21] A.K. Shukla, M.K. Ravikumar, M. Neergat, K.S. Gandhi, J. Appl. Electrochem. 29 (1999) 129–132.
[22] X. Ren, S.C. Thomas, P. Zelenay, S. Gottesfeld, J. Power Sources 86 (2000) 111–116.
[23] T.I. Valdez, S.R. Narayanan, N. Rohatgi, Proceedings of the Fifteenth Annual Battery Conference on Applications and Advances, IEEE, Long Island Beach, CA, USA, 2000, pp. 37–40.
[24] P. Argyropoulos, K. Scott, W.M. Taama, Electrochim. Acta 45 (2000) 1983–1998.
[25] P. Argyropoulos, K. Scott, W.M. Taama, J. Appl. Electrochem. 29 (1999) 661–669.
[26] J. Cruickshank, K. Scott, J. Power Sources 70 (1998) 40–47.
[27] J.T. Müller, P.M. Urban, W.F. Hölderich, J. Power Sources 84 (1999) 157–160.
[28] V. Gogel, T. Frey, Z. Yongsheng, K.A. Friedrich, L. Jörissen, J. Garche, J. Power Sources 127 (2004) 172–180.
[29] A.K. Shukla, C.L. Jackson, K. Scott, G. Murgia, J. Power Sources 111 (2002) 43–51.
[30] J. Divisek, J. Fuhrmann, K. Gärtner, R. Jung, J. Electrochem. Soc. 150 (6) (2003) A811–A825.
[31] Z.H. Wang, C.Y. Wang, J. Electrochem. Soc. 150 (4) (2003) A508–A519.
[32] A.A. Kulikovsky, Electrochem. Commun. 5 (2003) 530–538.
[33] A. Simoglou, P. Argyropoulos, E.B. Martin, K. Scott, A.J. Morris, W.M. Taama, Chem. Eng. Sci. 56 (2001) 6761–6772.
[34] A. Simoglou, P. Argyropoulos, E.B. Martin, K. Scott, A.J. Morris, W.M. Taama, Chem. Eng. Sci. 56 (2001) 6773–6779.
[35] A. Siebke, PhD Thesis, VDI Verlag GmbH, Düsseldorf, Germany, 2003.
[36] P. Argyropoulos, K. Scott, W.M. Taama, J. Power Sources 87 (2000) 153–161.
[37] S.R. Narayanan, T.I. Valdez, Electrochem. Soc. Proc. 2001 (4) (2001).
[38] K. Sundmacher, T. Schultz, S. Zhou, K. Scott, M. Ginkel, E.D. Gilles, Chem. Eng. Sci. 56 (2001) 333–341.
[39] S. Zhou, T. Schultz, M. Peglow, K. Sundmacher, Phys. Chem. Chem. Phys. 3 (2001) 347–355.
[40] A. Oedegaard, S. Hufschmidt, R. Wilmshoefer, C. Hebling, Fuel Cells 4 (3) (2004) 219–224.
[41] A.A. Kulikovsky, Electrochem. Commun. 4 (2002) 939–946.
[42] X. Ren, W. Henderson, S. Gottesfeld, J. Electrochem. Soc. 144 (9) (1997) L267–L270.
[43] X. Ren, T.E. Springer, S. Gottesfeld, J. Electrochem. Soc. 147 (1) (1997) 92–98.
[44] W. Vielstich, Handbook of Fuel Cells, vol.1, John Wiley and Sons Ltd., Chichester, United Kingdom, 2003 (Chapter 4).
[45] T.E. Springer, T.A. Zawodzinski, S. Gottesfeld, J. Electrochem. Soc. 138 (8) (1991) 2334–2342.
[46] H. Wang, T. Löffler, H. Baltruschat, J. Appl. Electrochem. 31 (2000) 759–765.
[47] H. Dohle, J. Divisek, J. Mergel, H.F. Oetjen, C. Zingler, D. Stolten, J. Power Sources 105 (2002) 274–282.
[48] J.-T. Wang, S. Wasmus, R.F. Savinell, J. Electrochem. Soc. 143 (4) (1996) 1233–1239.
[49] V.M. Barragán, A. Heinzel, J. Power Sources 104 (2002) 66–72.
[50] Z. Qi, A. Kaufman, J. Power Sources 110 (2002) 177–185.
[51] S. Shimpalee, S. Dutta, Numer. Heat Transf., Part A 38 (2000) 111–128.
[52] J.T. Müller, PhD Thesis, Shaker Verlag, Aachen, Germany, 2000.
[53] R. Jiang, C. Rong, D. Chu, J. Power Sources 126 (2004) 119–124.